Available online at www.sciencedirect.com
ScienceDirect
ELSEVIER
Composites Science and Technology 67 (2007) 720–727
COMPOSITES SCIENCE AND TECHNOLOGY
www.elsevier.com/locate/compscitech

In situ synthesis method and damping characterization of magnesium matrix composites

Zhang Xiuqing *, Wang Haowei, Liao Lihua, Ma Naiheng

Department of Materials Science and Engineering, State Key Laboratory of Metal Matrix Composites, Shanghai Jiao Tong University, Shanghai 200030, China

Received 25 February 2005; received in revised form 14 April 2006; accepted 24 April 2006
Available online 27 June 2006

Abstract

Magnesium matrix composites reinforced with 8 wt% TiC was in situ synthesized using remelting and dilution technique. X-ray diffraction analysis revealed the presence of TiC phase in sintered block and magnesium matrix composites. Uniform distribution of fine TiC particulates in matrix material was obtained through microstructure characterization. The results of damping characterization revealed that damping capacity of materials is independent of frequency, but dependent on strain and temperature. There were damping peak in damping–strain curve, which is due to the foul and tangle of dislocations. There were two damping peaks at damping–temperature curve under respective temperature of 130 °C and 240 °C. The former damping peak of magnesium matrix composites is due to dislocation motion, and the latter is due to interface and grain boundary sliding. Generally, damping capacity of magnesium matrix composites is higher than that of AZ91 magnesium alloy, which is due to the addition of TiC particulates.

Keywords: A. Metal-matrix composites (MMCs); E. Casting; B. Vibration; B. Microstructure

1. Introduction

It is well established that mechanical vibration causes much damage in automotive industry, architectural industry, bridge construction, machine housings and aerospace. What's more, noise is also accepted as pollution nuisance which damages human health. So it is important to seek for high damping capacity materials to eliminate or alleviate such damage. Pure magnesium is known to exhibit a very high damping capacity, but its ultimate tensile strength (UTS) is too low to be used widely [1,2]. Therefore, magnesium matrix composites (Mg-MMCs) reinforced with high strength reinforcements are a good candidate for realizing high damping: magnesium matrix being responsible for the high damping and reinforcements being responsible for the high-mechanical strength. So many researches have placed a showy emphasis on the damping capacity of Mg-MMCs. Schaller [3] studies the damping capacity of magnesium alloy and Mg-MMCs. His observations results revealed that the way of achieving high damping capacity and mechanical properties materials is the use of two-phase composites, in which each phase plays a specific role: damping or strengthening. And among the internal friction mechanisms, energy dissipation by dislocation movement is important. The research of Srikanth et al. [4] focuses on the relationship between the damping capabilities of the composite with the weight percentage of copper added to the matrix. Results of this study show that addition of copper increases the overall damping capacity of the AZ91 matrix. The study confirmed that the increase in damping is due to the increase in dislocation density and presence of plastic zone at the matrix–particulate interface. Trojanová et al. [5] investigated the internal stresses in AZ91 and WE54 magnesium alloys. Their results revealed that possible changes in the internal stresses and in the mobile dislocation density are considered to be responsible for the post-relaxation effect. A stress

* Corresponding author. Tel.: +86 21 6293 2569.
E-mail address: 740215@sjtu.edu.cn (Z. Xiuqing).

0266-3538/$ - see front matter
doi:10.1016/j.compscitech.2006.04.010

increment after stress relaxation in the temperature interval from 22 to150 °C indicates dynamic strain ageing. The observed anomalies are caused by the change in the concentration of solute atoms on dislocations with strain rate and temperature. Those results are advantageous to comprehend the damping characterization and mechanism. In order to more comprehend it, the damping of in situ Mg-MMCs would be investigated.

Generally, Mg-MMCs are synthesized using powder metallurgy, stir casting, pressure infiltration, etc. [6–8]. In situ synthesis is a new technique to prepare composites owing to many advantages, e.g. fine reinforcements, clean interface between matrix and reinforcement and good mechanical characterization [9,10]. Remelting and dilution is one of the in situ synthesis methods, and this method is made up of two steps. Firstly, sintered block consisting of reinforcements was prepared; secondly, sintered block was diluted into metal matrix melt to synthesize metal matrix composites. It is reckoned that remelting and dilution technique can be controlled easily, and its hoped to be applied in industry field widely. It is also important to select appropriate reinforcement that is wettable to metal matrix. As far as reinforcement concerned presently, TiC is good reinforcement because of its fine wetting property with magnesium matrix.

Accordingly, the primary aim of the present work was to in situ synthesize Mg-MMCs containing TiC ceramics particulate by using remelting and dilution technique. So the synthesized materials were examined for phase, microstructural and damping characterization.

2. Experimental procedures

The composite based on Mg–8 wt% TiC was prepared with the process of remelting and dilution (RD) technique. The process was composed of three steps which are to synthesize activated powder, to sinter the activated powder and to dilute and remelt the sintered block in molten magnesium.

In the experiment, the powder of Al, Ti and C whose purity degree is up to 99.5% and size is less than 75 μm were used at first. The composition of Al, Ti and C powder with mixture proportion of 50 wt%, 36.2 wt% and 14.8 wt% was milled. During the process the ratio of the ball and the powder was 5:1, and the milling time was 5 h.

The mixed powder was pressed into block with 30 mm diameter and 50 mm high under 15 MPa pressure. The relative density of un-sintered block was about 60–75%. Then, the block reacted at 1200 °C for 20 min in Ar gas atmosphere protection.

Magnesium ingot was superheated to 750 °C under the protection of $SF_6 + CO_2$ gas atmosphere in an iron crucible. The sintered block was added into the molten metal and then stirred at a speed about 250 rpm in order to dilute them to produce Mg-8 wt% TiC composites. Finally, the molten metal was poured into an iron sample mould. The composite was heat treated to T4 condition (14 h at 420 °C).

In order to identify the reaction products of the sintered block and the phase of Mg-MMCs, X-ray diffraction (XRD) analyses were carried out. With S-52 scanning electron microscope (SEM), the size and the amount of reinforcement were determined.

Damping capacity denotes the anti-vibration ability of materials. Generally speaking, damping capacity is described by the loss angle (φ), the loss factor (η), the reciprocal of quality factor (Q^{-1}). When the tan (φ) is lower than 0.1, these can interrelated by the equation: $\varphi = \tan\varphi = \eta = Q^{-1}$. Damping capacity measurements were performed on both composite and magnesium alloy specimens, adopting the three-point bending mode. The apparatus used was Mark IV dynamic mechanical thermal analyzer. The measurement conditions were frequency of approximately 0.1–20 Hz, maximum strain amplitude of approximately 0.01, temperature range between 288 and 523 K for magnesium alloy and Mg-MMCs specimens, and the heating rate was 2 K/min. The size of machined specimens was the 40 mm × 5 mm × 1.5 mm.

3. Experimental results

3.1. Phase analysis

Corresponding to the Mg-MMCs and the sintered block samples, the XRD results are shown in Fig. 1. The results revealed the presence of TiC phase in sintered block and Mg-MMCs sample. Alumina was also discovered in the sintered block. So the final phases in sintered block were Al, TiC and Al_2O_3 (see Fig. 1(a)). Compared to the sintered block, there was no Al_2O_3 phase in Mg-MMCs. The phases in Mg-MMCs were Mg, TiC and $Mg_{17}Al_{12}$.

3.2. Microstructure analysis

The results of microstructural characterization studies on sintered block and Mg-MMCs samples were discussed in terms of size and distribution of TiC particulates. The results of scanning electron micrographs revealed a uniform distribution of reinforcements in Mg-MMCs (see Fig. 2). The size of TiC particulates was about 0.2–1.0 μm. Microstructural characterization of sintered block consisted of white aluminum piece, white reinforcement spots and grey structure mixed with aluminum and reinforcement particles. Macrovoids were observed in the microstructure of sintered block. The presence of white banding $Mg_{17}Al_{12}$ phase was observed through scanning electron micrographs (see Fig. 2(b)). The microstructural characterization of composite material also revealed the formation of near defect free interface between reinforcements and matrix.

EDX analysis of Mg-MMCs is conducted on the area shown in Fig. 2(b). The results of EDX analysis revealed that element titanium is 8.67 wt%, and element aluminum

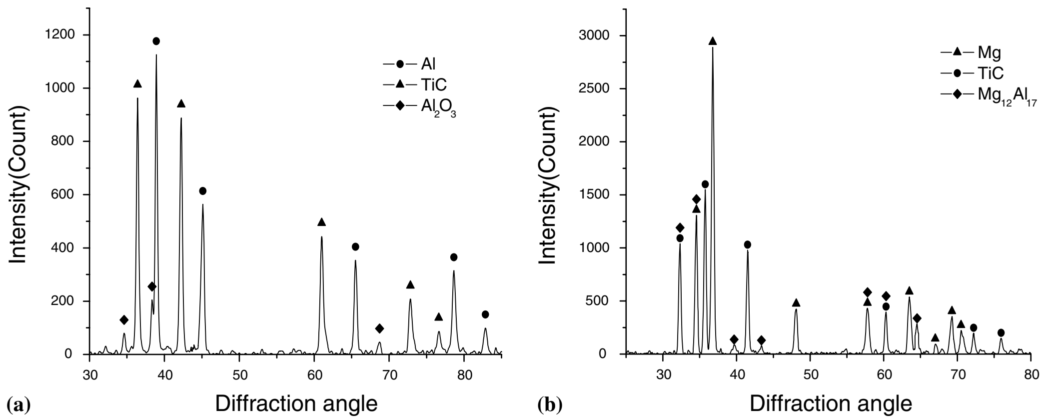

Fig. 1. X-ray diffraction patterns of samples: (a) prefabricated and (b) magnesium-based composite.

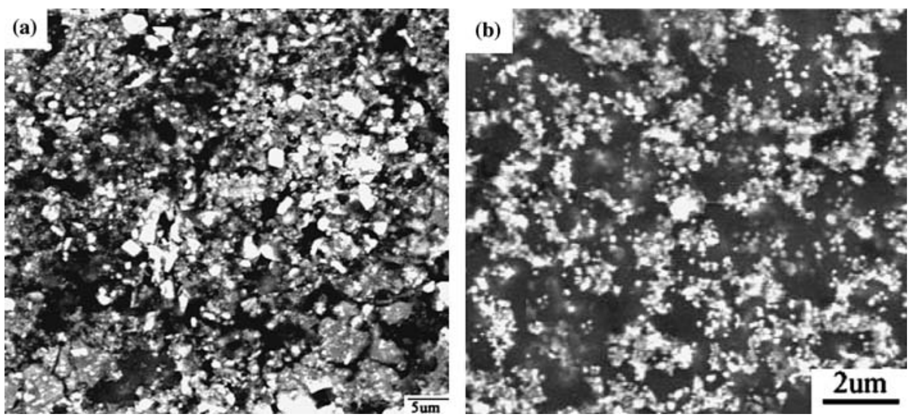

Fig. 2. SEM micrograph shows microstructure of: (a) sintered block and (b) Mg-MMCs.

is 6.91 wt% in Mg-MMCs (see Fig. 3). It can be calculated that there is 11.15 wt% reinforcement particulates in the Mg-MMCs because element titanium is being by mean of TiC in Mg-MMCs mainly. It can be calculated that the volume percent of reinforcement particulates in Mg-MMCs is about 4.24%. The weight present of aluminum in Mg-MMCs is according with the standard content of AZ91 magnesium alloy.

3.3. Damping capacity

Damping capacity of AZ91 magnesium alloy and Mg-MMCs was found to be independent of vibration frequency under lower stresses (0.01 MPa) and lower temperature (15 °C) (see Fig. 4(a)). Damping capacity of AZ91 magnesium alloy and Mg-MMCs increased when strain increased on low strain amplitude standard, but there was a damping peak in damping capacity curve of them when strain amplitude was about 3.0219×10^{-4} (see Figs. 4(b) and 5). And damping capacity of Mg-MMCs was higher than that of AZ91 magnesium alloy. Damping capacity of Mg-MMCs increased after heat treating (see Fig. 5).

Damping capacity of Mg-MMCs was found to be intensively dependent on the testing temperature, and it increased at different vibration frequency with increasing temperature. Moreover, it is observed that damping capacity of Mg-MMCs decreased when the vibration frequency increased, and the appearance of damping peak around 130 °C or 240 °C, respectively, at different vibration frequency such as 0.1 Hz, 0.5 Hz, 1.0 Hz and 2.0 Hz. The faster the vibration frequency was, the earlier the former damping peak formed (see Fig. 6).

4. Discussion

4.1. XRD analysis

During the sintering process, the mixed powder such as Al–Ti–C reacted. The reaction equation and its standard reacting free energy at 1400 K temperature are listed as follows [11,12]:

$$3\mathrm{Al} + \mathrm{Ti} \rightarrow \mathrm{TiAl_3} \quad \Delta G = -3.724\ \mathrm{kJ/mol} \tag{1}$$

$$\mathrm{TiAl_3} + \mathrm{C} \rightarrow 3\mathrm{Al} + \mathrm{TiC} \quad \Delta G = -74.02\ \mathrm{kJ/mol} \tag{2}$$

where the ΔG is the reacting free energy at 1400 K temperature. According to the reacting equation, aluminum acts as a reacting intermedium to facilitate the reaction between titanium and graphite. So the mixed powder reacts accord-

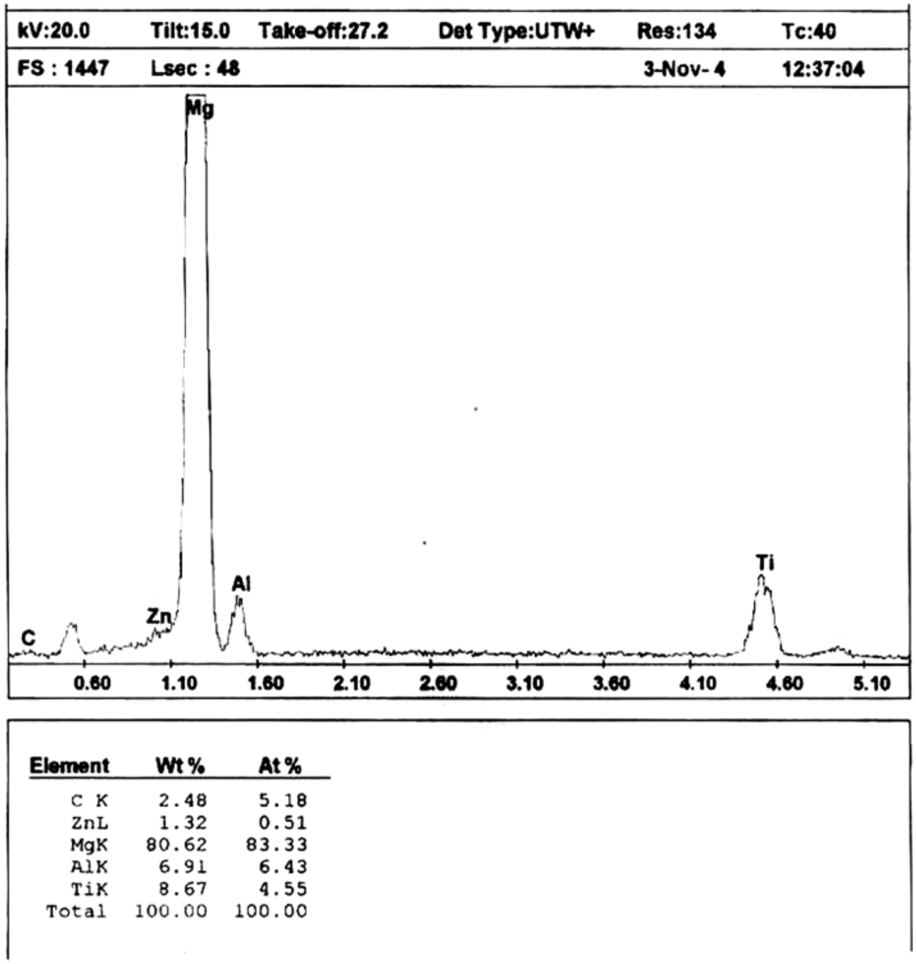

Element	Wt %	At %
C K	2.48	5.18
ZnL	1.32	0.51
MgK	80.62	83.33
AlK	6.91	6.43
TiK	8.67	4.55
Total	100.00	100.00

Fig. 3. EDX analyses of Mg-MMCs.

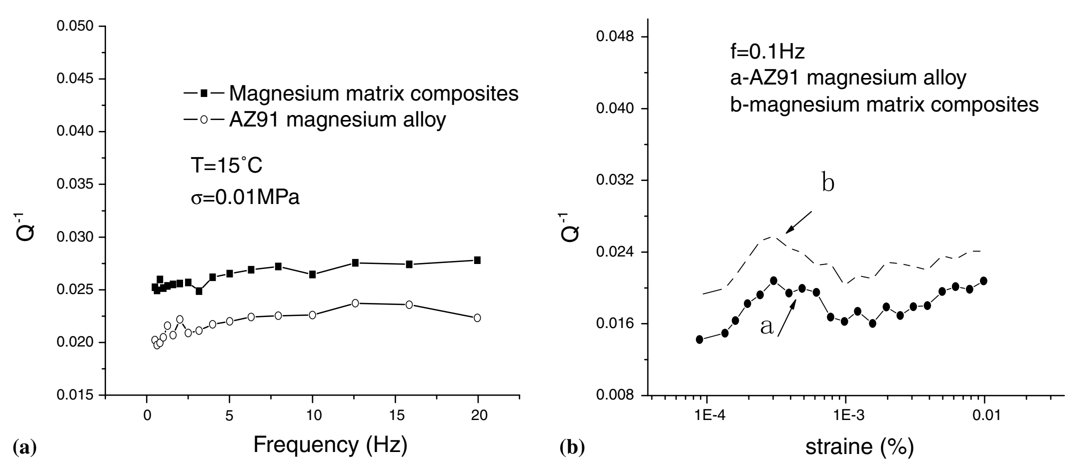

Fig. 4. Damping capacities of AZ91 magnesium alloy and Mg-MMCs: (a) corresponding to frequency and (b) corresponding to strain.

ing to the following reaction equation: Al + Ti + C = Al + TiC at 1400 K. The final products of sintered block are TiC and Al. The results of XRD confirm the presence of TiC and Al in sintered block.

Alumina is discovered in the sintered block because aluminum is oxidized during mixing and sintering process (see Fig. 1(a)). For its poor wettability to magnesium matrix, it cannot be observed in Mg-MMCs. Alumina deposits on the crucible bottom with fusing agent and impurity because the density of alumina is larger than that of magnesium. The presence of TiC in Mg-MMCs can be attributed to the good wettability between TiC and magnesium

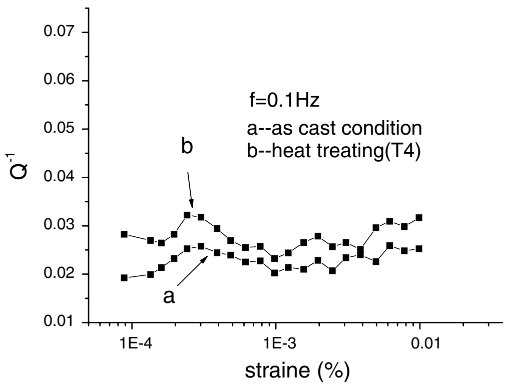

Fig. 5. Damping capacities of Mg-MMCs corresponding to heat treating.

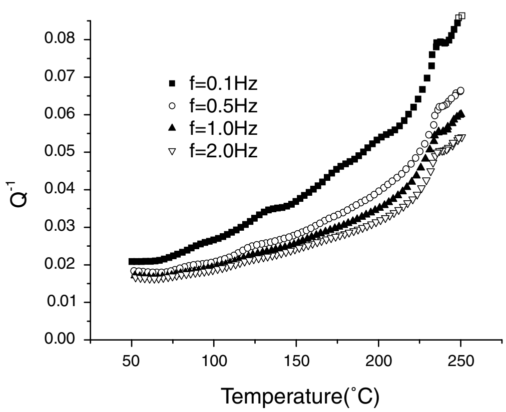

Fig. 6. Damping capacities of Mg-MMCs corresponding to temperature.

[13]. Aluminum being in sintered block diffuses into magnesium melt, and reacts with magnesium to turn into $Mg_{17}Al_{12}$ phase during solidification. The presence of $Mg_{17}Al_{12}$ phase in the composites sample is identified using XRD analysis (see Fig. 1(b)).

4.2. Microstructure analysis

Aluminum powder acts as an intermedium to accelerate the reaction of titanium and graphite during sintering process. The uniform distribution of TiC in sintered block can be attributed to: (i) uniform bending due to efficient ball milling and (ii) the hindrance function of aluminum to reinforcements. Microstructural characterization of sintered block reveal some macrovoids (see Fig. 2(a)), which is due to the low relative density of un-sintered block that is about 60–75%.

In the present study, the uniform distribution of TiC particulates in Mg-MMCs can be attributed to minimal agglomeration of reinforcements, when it melted into magnesium matrix. It can also be attributed to judicious selection of stirring parameters, which ensured uniform incorporation of reinforcements particulates in magnesium matrix melt. Microstructural characterization of the composite reveal a near defect free interface formed between reinforcements and matrix (see Fig. 2(b)), which is assessed in terms of interfacial debonding and microvoids at the particulate–matrix interface. The presence of minimal porosity in the composite (see Fig. 2(b)) can be attributed to: (i) good compatibility between magnesium–TiC ceramic system and (ii) the good casting properties of the AZ91 magnesium alloy.

Microstructural characterization revealed that the average size of TiC particulates is 0.2–1.0 μm (see Fig. 2), and this can be attributed to the efficient ball milling and the severe reaction between Ti and C.

4.3. Damping characterization

At low temperatures, for many metallic materials two damping mechanisms are usually considered. The first the dynamic damping, is frequency dependent but independent of strain amplitude; the second, the break-away damping, was found to depend on the strain amplitude. The damping capacity of materials can be expressed as follows [14,15]:

$$Q^{-1} = Q_{\mathrm{f}}^{-1} + Q_{\mathrm{a}}^{-1} \tag{3}$$

$$Q_f^{-1} = \frac{C_1 \rho f^2}{b^2} \tag{4}$$

$$Q_a^{-1} = C_2 \frac{\rho b^2}{\varepsilon_0} \exp\left(-\frac{C_3}{\varepsilon_0}\right) \tag{5}$$

where Q_{f}^{-1} is the strain amplitude independent component. The component Q_{a}^{-1} depends on the strain amplitude and it is determined usually by dislocation vibrations. C_1, C_2, C_3 are numerical factors, ρ the dislocation density, b the Burgers vector, ε_0 the strain amplitude, and f the vibration frequency. In our research, the materials belong to static state anelasticity under low stress [14], so the damping capacity of the composites and magnesium alloy is independent of frequency (see Fig. 4(a)).

We put the emphasis on the break-away damping. In metal matrix, dislocation is pinned by the strong pinning points such as TiC particulates and the weak pinning points such as solution atoms (see Fig. 9). So the dislocation behaves like an elastic vibration string. At low strain amplitude, dislocation string L_i (L_1, L_2 and L_3) vibrates to and fro to dissipate energy (see Fig. 9(b)–(c)). In the region, the damping capacity of these composites is only weakly dependent on strain amplitude. It improves slowly when strain amplitude increase (see Figs. 4, 5). With the increasing of applied stress, dislocation string breaks away the weak pinning, and the unpinning of dislocation occurs (see Fig. 9(d)–(f)). So the break-away damping capacity generates. In our research, the applied stress load is too low to unpin the dislocation, so damping capacity of these materials increases slowly at the all strain amplitude. But the unpinning process of dislocations also generates when testing temperature increase. So the presence of the damping peak at about 130 °C is contributed to the avalanche effect of anchoring of dislocation.

Simultaneously, dislocation moves and then crossing and interaction of dislocation occur, which leads to the tangle of dislocations. So some dislocations cannot move again, and the effective length of chord sympathetic vibration dislocations becomes shorter than that of the former. Correspondingly, damping capacity of materials decrease after strain amplitude increases to a special value, so there is a strain peak in damping–strain curve of AZ91 magnesium alloy and Mg-MMCs at about 3.0219×10^{-4} (see Figs. 4, 5). This result is the same as that of study on Al–17Si–xLa alloys [4,16].

Metal matrix composites reinforced by particulates will cause high residual stresses around the particulates because of the distant discrepancy of thermal expansion coefficient between magnesium and reinforcements, which are responsible for the generation of high dislocation density in matrix [17,18] (see Fig. 7). The increase in the dislocation density is given as follows [16]:

$$\rho = \frac{9.6\Delta\alpha\Delta T V_p}{bd} \quad (6)$$

where $\Delta\alpha$ is the difference of thermal expansion coefficient between matrix alloy and reinforcements, ΔT is difference between working temperature and final temperature, b is the Burger vector, V_p is the volume fractions, and d is the diameter of reinforcements. In our study, $\Delta\alpha$ is $20.5 \times 10^{-6}\,\mathrm{K}^{-1}$, ΔT is 280 K, b is 0.32094 nm, d is average 0.6 μm, and V_p is 3.1%. So the dislocation density of composites is $8.87 \times 10^{10}\,\mathrm{mm}^{-2}$ corresponding to 8 wt%TiC/AZ91 composites. With the increasing of TiC particulates, the dislocation densities of composites increase (see Fig. 7). According to Eq. (5), damping capacity of Mg-MMCs is higher than that of AZ91 magnesium alloy (see Figs. 4 and 5).

Heat treated as T4, the dislocation density of Mg-MMCs becomes low, but these processes may also result in an increase in the effective length of the shorter dislocation segments, and the number of movable dislocation is larger (see Fig. 8). According to Eq. (5), the damping capacity of Mg-MMCs increases after heat-treatment (see Fig. 5) [19,20].

It has been suggested that the grain boundary and the interface between the reinforcement and matrix may play an important role in the damping behavior of composite materials. As the stress is applied, the interface and grain boundary sliding to dissipate energy (see Fig. 10). The energy dissipated in the boundaries is mainly dependent on the temperature, the shear stress, and the anelastic shear strain [21,22]. With the temperature increasing, besides energy dissipating due to chord sympathetic vibration of dislocations, which results in the damping peak at about 130 °C, much energy was dissipated between the movable interfaces of the composites. So the damping capacity was greatly improved. The presence of damping peak around 240 °C would were observed at damping–temperature curve under several vibration frequencies (see Fig. 6). The damping peak at 240 °C is contributed to the movable interfaces between magnesium matrix and TiC ceramic. Interfaces may affect the damping behavior of the materials because they are two-dimensional defects, where the crystal structure is distorted locally. A theory regarding the contribution of the reinforcements–matrix interface to damping

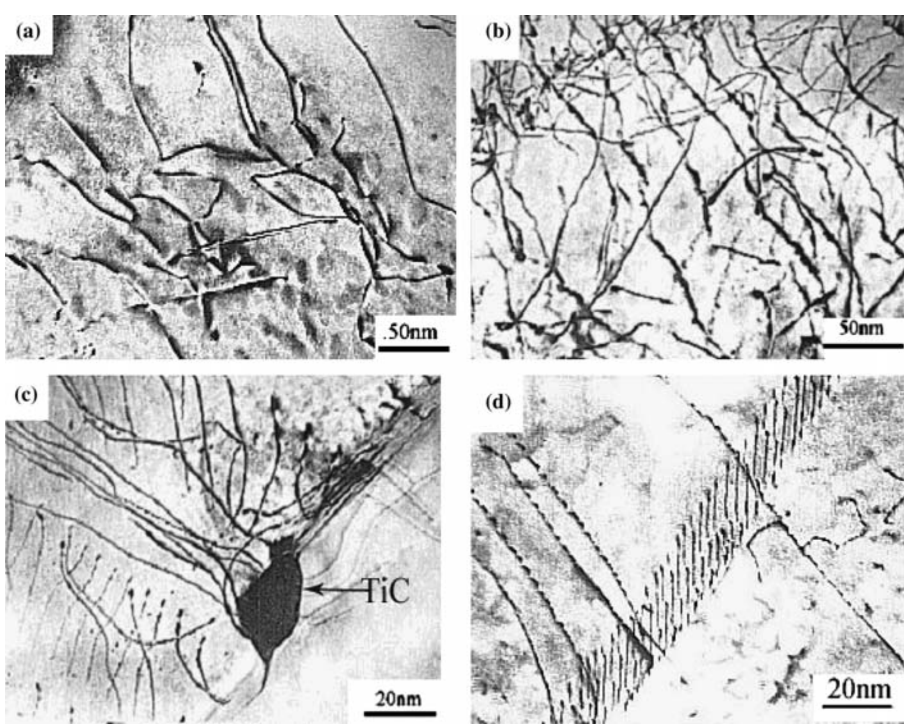

Fig. 7. The dislocation arrangement in materials: (a) AZ91 magnesium alloy; (b–d) 8 wt%TiC/AZ91 composites.

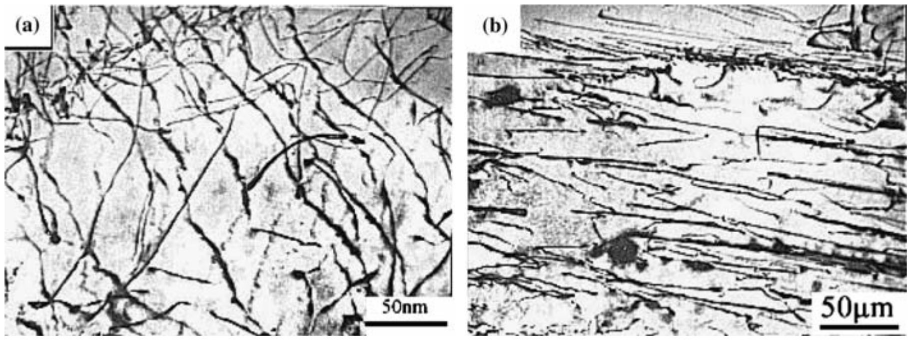

Fig. 8. The dislocation of 8 wt%TiC/AZ91 composites: (a) F and (b) T4.

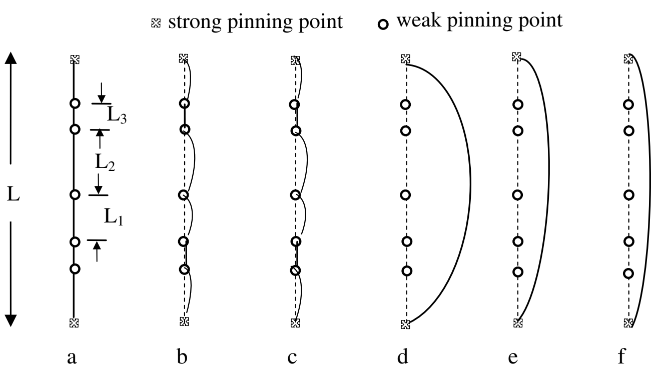

Fig. 9. The damping mechanism according to dislocation movement.

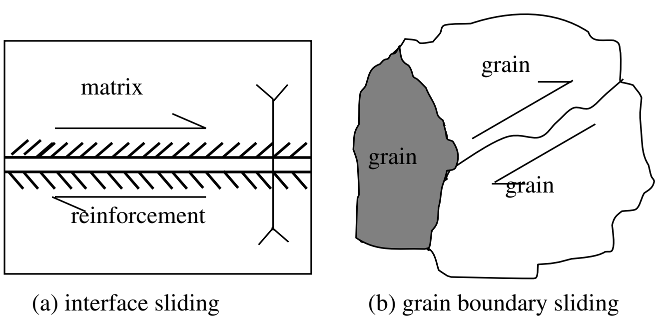

Fig. 10. The damping mechanism of interface sliding and grain boundary sliding.

has been offered by Schoeck [23,24]. Assuming a viscous boundary to exist at the interface at high temperature, the contribution to damping is approximately given by:

$$Q^{-1} \approx [4.5(1-\gamma)V_f\ ]/[\pi^2(2-\gamma)] \tag{7}$$

where γ is Poisson's ratio and V_f is volume fraction of reinforcements particulates. In our research, γ is 0.35, so the Q^{-1} is about 5.57×10^{-3}. This value is consistent with the observed increase in damping at elevated temperatures.

The interface damping can be explained by elastic thermodynamic damping mechanism. The elastic thermodynamic damping mechanism was proposed by Zener [25] based on the fact that energy is dissipated by the irreversible heat flow within a material caused by stress induced thermal gradients. Whenever a material is stressed in a reversible adiabatic process (constant entropy), there is always a change in temperature, which may be very small. This phenomenon is the well-known thermoelastic effect. Heat conducts from the high temperature region to low temperature region and as a consequence of second law of thermodynamics entropy is produced which is manifested as a conversion of useful mechanical energy into heat. The contribution to damping due to thermoelastic effect is given by [25]:

$$\mathrm{Tan}\,\varphi = \frac{E_u\alpha^2T_0\omega\tau}{C\sigma(1+\omega^2\tau^2)} \tag{8}$$

where $\tau = a^2C\sigma/\pi^2K\mathrm{th}$, E_u is the unrelaxed elastic modulus, α is the coefficient of thermal expansion, T_0 is the absolute temperature, $C\sigma$ is the specific heat/unit volume, ω is the angular frequency, τ is the relaxation time, a is the beam thickness, and Kth is the thermal conductivity. The described thermoelastic contribution to damping capacity at certain temperatures is shown as Fig. 6.

5. Conclusion

1. Remelting and dilution technique can be used to in situ synthesize TiC particulates reinforced Mg-MMCs successfully.
2. Final products of sintered block are TiC, Al_2O_3 and Al, the size of the in situ synthesis TiC particulates is about 0.2–1.0 μm. The results of XRD confirm the presence of TiC in sintered blocks and Mg-MMCs.
3. Microstructural characterization reveals the uniform distribution of TiC ceramic particulates in magnesium matrix, which can be attributed to: (i) minimal agglomeration of reinforcements, (ii) good wettability between TiC and magnesium and (iii) judicious selection of stirring parameters.
4. Under low applied stress load, damping capacity of materials is independent of vibration frequency but dependent on strain. It increases as strain amplitude rising, and there is a strain peak in damping–strain curve, which was due to the motion and tangle of dislocations.

5. Damping capacity of Mg-MMCs increases after heat-treating because of the increasing of the effective length of vibration dislocations, and the increasing of the number of mobile dislocations.
6. Damping capacity of Mg-MMCs was higher than that of AZ91 magnesium alloy, which is due to the high dislocation density in Mg-MMCs caused by the addition of TiC particulates.
7. Damping capacity of Mg-MMCs is dependent on temperature intensively, and they increase as temperature ascending. Under different vibration frequency, there are respective temperature peak at damping–temperature curve around 130 °C and 240 °C. The former temperature peak is due to dislocation motion, and the later is due to interface sliding.

Acknowledgement

The authors thank State Key Laboratory of Metal Matrix Composites for providing the testing.

References

[1] Luo Alan A. Recent magnesium alloy development for automotive powertrain applications. Mater Sci Forum 2003;419–422(1):57–66.
[2] Smoot Perry R. High specific modulus magnesium matrix composite. In: Proceedings of the National SAMPE technical conference, advanced materials: looking ahead to the 21st century, vol. 22; 1990. p. 825–33.
[3] Schaller R. Metal matrix composites, a smart choice for high damping materials. J Alloy Compd 2003;355(1–2):131–5.
[4] Srikanth N, Gaofeng CH, Gupta M. Enhanced damping of a magnesium alloy by addition of copper. J Alloy Compd 2003;352 (1–2):106–10.
[5] Trojanova Z, Lukac P, Milicka K, Szaraz Z. Characterisation of dynamic strain ageing in two magnesium alloys. Mater Sci Eng A 2004;387–389(1):80–3.
[6] Hassan SF, Gupta M. Development of a novel magnesium/nickel composite with improved mechanical properties. J Alloy Compd 2002;335(1–2):L10–5.
[7] Manoharan M, Lim SCV, Gupta M. Application of a model for the work hardening behavior to Mg/SiC composites synthesized using a fluxless casting process. Mater Sci Eng A 2002;A333(1–2):243–9.
[8] Ferkel H, Mordike BL. Magnesium strengthened by SiC nanoparticles. Mater Sci Eng A 2001;A298(1–2):193–9.
[9] Wang HY, Jiang QC, Li XL, Wang JG. In situ synthesis of TiC/Mg composites in molten magnesium. Scripta Mater 2003;48(9):1349–13549.
[10] Xun ZQ, Zhang D, Ding J, Fan TX, Lv WJ. Research development of in-situ magnesium matrix composites and the in-situ reaction thermodynamics of the reaction systems. Mater Sci Eng 2002;20(4):579–84.
[11] Tang JX, Cheng JH, Zeng ZQ, Miao HZ. Diffusion path and reaction mechanism between Ti and B_4C. J Inorg Mater 2000;15(5):884–8.
[12] Ye DL. Thermodynamics date handbook of practical inorganic matter. Beijing: Metallurgical Industry Press; 1981.
[13] Contreras A, Leon CA, Drew RAL, Bedolla ES. Wettability and spreading kinetics of Al and Mg on TiC. Scripta Mater 2003;48(12): 1625–30.
[14] Granato A, Lücke K. Theory of mechanical damping due to dislocations. J Appl Phys 1956;27(6):583–93.
[15] Granato A, Lücke K. Application of dislocation theory to internal friction phenomena at high frequencies. J Appl Phys 1956;27(7): 789–805.
[16] Yi HK, Liu ZT, Li FH, Zhang D. Investigation on room temperature damping vs strain amplitude behaviors of hypereutectic Al-17Si–xLa alloys. Funct Mater 2003;34(5):525–8.
[17] Jia DC. Influence of SiC particulate size on the microstructural evolution and mechanical properties of Al–6Ti–6Nb matrix composites. Mater Sci Eng A 2000;289(1):83–90.
[18] Carreno-Morelli E, Urreta SE, Schaller R. Mechanical spectroscopy of thermal stress relaxation in aluminum alloys reinforced with short alumina fibres. Phys Status Solidi A – Appl Res 1998;167(1):61–9.
[19] Ma CJ, Zhang D, Ding WJ, Wang QD. Damping capacity of SiC_w/ MgLiAl composites. J Mater Sci Lett 2001;20(4):327–9.
[20] Chmelik F, Lukac P, Kiehn J, Mordike LB, Kainer KU, Langdon GT. Characteristics of thermal cycling in a magnesium alloy composite. Mater Sci Eng A 2002;325(1–2):320–3.
[21] Liu YH, Li JF, Yang GC, Lu YL. High damping functional materials prepared by spray deposition. J Mater Process Technol 2000;106: 94–8.
[22] Lavernia EJ, Perez RJ, Zhang J. Damping behavior of discontinuously reinforced Al alloy metal-matrix composites. Metall Mater Trans A: Phys Metall Mater Sci 1995;26A(11):2803–18.
[23] Schoeck G. Internal friction due to precipitation. Phys Status Solidi 1969;32(2):651–8.
[24] Lavernia EJ, Baram J, Gutierrez E. Precipitation and excess solid solubility in Mg–Al–Zr and Mg–Zn–Zr processed by spray atomization and deposition. Mater Sci Eng A – Struct Mater Properties Microstruct Process 1991;A132(1–2):119–33.
[25] Zener C. In: Elasticity and anelasticity of metals. Chicago (IL): The University of Chicago; 1948.